William R. Wiley
EMSL
Environmental Molecular Sciences Laboratory

EMSL Report

March/April 2006

The W.R. Wiley Environmental Molecular Sciences Laboratory (EMSL) is a U.S. Department of Energy (DOE) national scientific user facility located at Pacific Northwest National Laboratory (PNNL) in Richland, Washington. EMSL is operated by PNNL for the DOE Office of Biological and Environmental Research. At one location, EMSL offers a comprehensive array of leading-edge resources in six research facilities.

Access to the capabilities and instrumentation in EMSL facilities is obtained on a peer-reviewed proposal basis. Users are participants on accepted proposals. EMSL staff members work with users to expedite access to the facilities and scientific expertise. The Bimonthly Report documents research and activities of EMSL staff and users.

Research Highlights

Imaging Adsorbate O-H Bond Cleavage: Methanol on $TiO_2(110)$

ZR Zhang,[(a)] O Bondarchuk,[(a)] JM White,[(a)] BD Kay,[(b)] and Z Dohnálek[(b)]

(a) University of Texas, Austin, Texas

(b) Pacific Northwest National Laboratory, Richland, Washington

The wide-ranging importance of titanium oxide (TiO_2) in heterogeneous catalysis, photocatalysis, sensor applications, and hydrogen production using solar cells has made this surface one of the most extensively studied. Despite this extensive research attention, the interactions of well-characterized TiO_2 surfaces with simple molecules that participate in a number of catalytic reactions on TiO_2 are not well understood. This study focused on further developing our understanding these fundamental reaction mechanisms with the intent of further exploiting the properties of this technologically important material.

The thermal and photocatalytic oxidation of simple alcohols has been extensively studied on TiO_2 surfaces as a prototype for the catalytic oxidation of organic contaminants. Among them, methanol (CH_3OH), which is one of the simplest organic molecules, is often adopted as a probe. Experiments have shown that both molecular and dissociative adsorption take place on defective rutile $TiO_2(110)$ surfaces. Methanol dissociation occurs primarily on bridge-bonded oxygen vacancy (BBOV) defect sites with some evidence for CH_3OH dissociation at non-defect sites as well. First-principle calculations show that on a stoichiometric surface, the dissociative adsorption of CH_3OH can occur via both O-H and C-O bond scission and that it is slightly favored over molecular adsorption. However, the atomic level understanding of these systems is still missing.

Scanning tunneling microcopy (STM) is an ideal analytical tool that allows researchers to track adsorbates on different surface sites. In this study, we employed *in situ* STM to follow the adsorption and dissociation of CH_3OH on BBOVs of $TiO_2(110)$. Experiments were performed in an ultrahigh vacuum variable-temperature STM chamber. Figure 1 shows a set of STM images obtained from the same $TiO_2(110)$ area before and after dosing with CH_3OH at 300 K. Figure 1a represents a clean surface before CH_3OH adsorption. The bright rows on Figure 1a are identified as the fivefold coordinated Ti^{4+} ions; the dark rows are the bridge-bonded oxygen (BBO) ions. The bright spots between the Ti^{4+} rows are assigned to BBOVs, believed to act as the primary dissociation centers for the alcohols. Statistically, the number density of

BBOVs on this surface is about 8% with respect to the number of Ti^{4+}. The magnified images (insets in Figure 1) highlight the position of six BBOV sites (marked by yellow circles in Figure 1a) to illustrate the processes observed during CH_3OH adsorption.

The surface after an 80-s methanol dose is shown in Figure 1b. The CH_3OH adsorption-induced features appear as bright features on the BBOVs. The spatial location of adsorption sites becomes apparent from comparison of the magnified areas in the insets of panels "a" and "b" in Figure 1. The pattern of the bright features (marked with blue circles on the of panel b inset) is the same as the BBOV pattern on the clean surface (yellow circles on the panel a inset), indicating that CH_3OH preferentially adsorbed on the BBOVs. Comparing line profiles along the [001] direction shows that the bright features are 0.8 Å higher than BBOVs and that the CH_3OH-induced bright features have their maxima located on the original BBOV sites, but are asymmetric. This finding suggests that these features originate from two different chemical species present on neighboring BBO sites, in accord with the previously observed formation of hydroxyl and methoxy species resulting from the dissociative adsorption of CH_3OH. This process is shown schematically in Figure 1f.

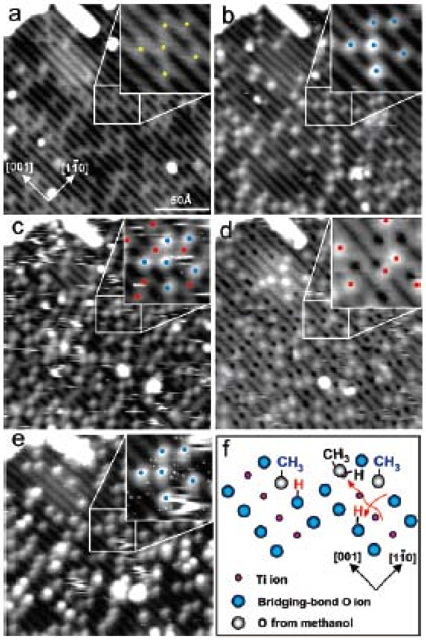

Figure 1. STM images of same area before and after adsorption of CH_3OH on $TiO_2(110)$ at 300 K: (a) bare surface; (b) after 80-s exposure to CH_3OH ; (c) after 110-s exposure to CH_3OH ; (d) taken on (c) after spontaneous tip change; (e) after high bias sweep of (c); (f) schematic of the adsorption process.

We conclude that CH_3OH dissociates on BBOVs via O-H bond scission. In the case of C-O bond scission, the hydroxyl rather than the methoxy group would appear on the original BBOV sites. At high coverage levels (Figure 1c), all the hydroxyl groups appear to be spatially separated from the methoxy groups (bright/gray; 1:1) as they migrated away from their original geminate sites. We propose that diffusing CH_3OH molecules assist hydroxyl migration, most likely through proton "hopping." At CH_3OH coverage below the BBOV coverage, the CH_3OH molecules diffusing on Ti^{4+} rows dissociate after encountering an empty BBOV. At CH_3OH coverage exceeding the BBOV coverage, excess CH_3OH is mobile and leads to the observed dramatic increase in hydroxyl migration. Figure 2 shows a schematic model for CH_3OH-assisted hydroxyl migration on $TiO_2(110)$. Repeated imaging of the same area provides additional evidence for the high mobility of hydroxyls at high CH_3OH coverage. We believe this mobility is facilitated by molecular CH_3OH diffusing along the Ti^{4+} rows: as much as 40% of the hydroxyls changed position in two consecutive images (3 min).

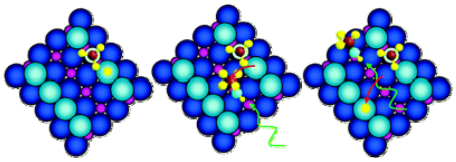

Figure 2. A schematic for methanol-assisted hydroxyl migration on $TiO_2(110)$.

In summary, we present the first atomically resolved images of dissociative methanol adsorption on BBO vacancies of $TiO_2(110)$. Imaging of the same area before and after adsorption allowed us to establish that the dissociation proceeds via O-H bond scission. At CH_3OH coverage below the BBO vacancy coverage, the methoxy and hydroxyls occupy primarily neighboring BBO sites. At higher levels of coverage, facile hydroxyl migration assisted by mobile, Ti^{4+}-bound CH_3OH molecules is observed.

This research is described in more detail in Zhang et al. 2006.

Citation

Zhang ZR, O Bondarchuk, JM White, BD Kay, and Z Dohnalek. 2006. "Imaging Adsorbate O-H Bond Cleavage: Methanol on $TiO_2(110)$." *Journal of the American Chemical Society* 128(13):4198-4199.

The Effect of Calcium on Aqueous Uranium(VI) Speciation and Adsorption to Ferrihydrite and Quartz

PM Fox,[(a)] *JA Davis,*[(a)] *and JM Zachara*[(b)]

(a) U.S. Geological Survey, Menlo Park, California
(b) Pacific Northwest National Laboratory, Richland, Washington

This study demonstrated that the presence of calcium at environmentally relevant concentrations significantly reduces the amount of uranium adsorbed on ferrihydrate and quartz and increases the concentration of soluble and mobile uranium(VI) species.

Recent studies of uranium(VI) geochemistry have focused on the potentially important role of the aqueous species, $CaUO_2(CO_3)_3^{2-}$ and $Ca_2UO_2(CO_3)_3^0(aq)$, on inhibition of microbial reduction and uranium(VI) aqueous speciation in contaminated groundwater. However, to our knowledge, there have been no direct studies of the effects of these species on uranium(VI) adsorption by mineral phases. The sorption of uranium(VI) on quartz and ferrihydrite was investigated in $NaNO_3$ solutions equilibrated with either ambient air (430 ppm CO_2) or 2% CO_2 in the presence of 0, 1.8, or 8.9 mM Ca^{2+}. Under conditions in which the $Ca_2UO_2(CO_3)_3^0(aq)$ species predominates uranium(VI) aqueous speciation, the presence of calcium in solution lowered uranium(VI) adsorption on quartz from 77% in the absence of calcium to 42% and 10% at calcium concentrations of 1.8 and 8.9 mM, respectively. Uranium(VI) adsorption to ferrihydrite decreased from 83% in the absence of calcium to 57% in the presence of 1.8 mM calcium. Surface complexation model predictions that included the formation constant for aqueous $Ca_2UO_2(CO_3)_3^0(aq)$ accurately simulated the effect of Ca^{2+} on uranium(VI) sorption onto quartz and ferrihydrite within the thermodynamic uncertainty of the stability constant value. This study confirms that Ca^{2+} can have a significant impact on the aqueous speciation of uranium(VI), and consequently, on the sorption and mobility of uranium(VI) in aquifers.

Microscopic View of Strontium Interactions in Minerals

GM Bowers,[a] AS Lipton,[b] MC Davis,[a] R Ravella,[a] S Komarneni,[a] and KT Mueller[a]

(a) Pennsylvania State University, University Park, Pennsylvania

(b) Pacific Northwest National Laboratory, Richland, Washington

Characterization of strontium in phyllosilicate minerals with solid-state nuclear magnetic resonance spectrometry (NMR) will contribute to an understanding of strontium/mineral interactions in soils exposed to leaking waste tanks, thus enabling the design of better models for predicting the fate of strontium in the environment and better cleanup technologies.

The interactions of strontium with clay minerals and zeolites are not well understood and must be researched so accurate models for predicting the environmental fate of radioactive strontium-90 released from sites such as Hanford can be developed. Solid-state NMR spectrometry is a useful tool for probing the molecular structure of materials, including the interactions of cations sorbed by mineral systems. However, there is only one NMR active isotope of strontium (i.e., strontium-87) and the direct study of strontium with solid-state NMR is experimentally challenging. Strontium-87 has similar chemistry to strontium-90 and is a quadrupolar nucleus (I = -9/2) with a low natural abundance (~7%), a low gyromagnetic ratio ($\gamma = -1.163 \times 10^{7}\ 1^{-1}T^{-s}$), and large quadrupolar coupling constants (14-25 MHz) (Larsen et al. 2000; Bastow 2002; Bowers et al. 2006). These factors contribute to a lack of sensitivity that must be overcome to perform time-efficient studies of strontium in natural samples, such as environmentally relevant clay minerals and zeolites.

In our ongoing studies at PNNL on the 21.14-tesla (T) (^{1}H resonance frequency of 900 MHz) instrument, we are using sensitivity-enhancing techniques to characterize the local electromagnetic environment of strontium nuclei in mineral systems. We have shown in recent work that the 21.14-T (900-MHz) field strength provides an order-of-magnitude enhancement to the signal-to-noise ratio for strontium-87 experiments and that quadrupolar Carr Purcell Meiboom Gill (QCPMG) analysis adds an additional order of magnitude (Bowers et al. 2006). Unfortunately, these enhancements were insufficient to observe strontium in complex minerals. In the past year, we were able to demonstrate that adding the double frequency sweep (DFS) preparatory scheme results in up to an additional fivefold enhancement to the signal-to-noise ratio (Figure 1), thereby permitting the detection of strontium resonances in soil minerals.

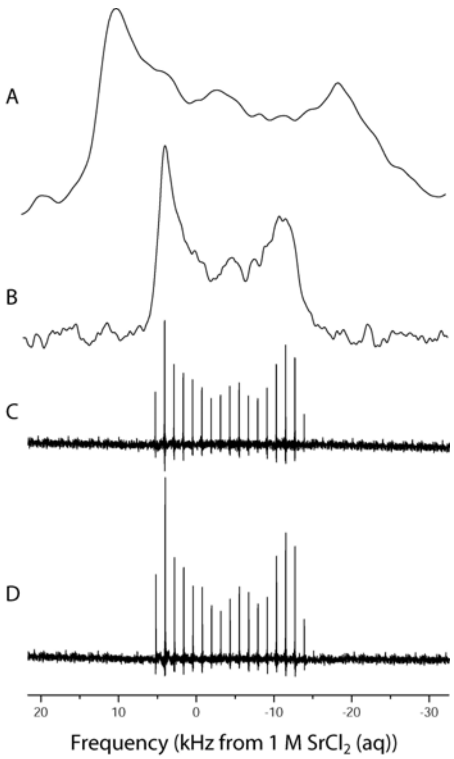

Figure 1. Strontium carbonate strontium-87 NMR spectra: (A) static echo at 11.74 T (800 MHz), (B) static echo at 21.14 T scaled by 1/37, (C) QCPMG at 21.14 T (900-MHz) scaled by 1/275, (D) DFS-QCPMG at 21.14 T scaled by 1/826.

With DFS-QCPMG at 21.14 T (900 MHz), we were able to perform solid-state NMR studies of strontium in additional inorganic and organic systems, where these studies were impossible with QCPMG analysis alone. One important conclusion from our data is that water-strontium interactions have a profound effect on strontium-87 NMR spectra; in fact, we have been unable to observe strontium in any system where there is water in the strontium hydration sphere (Figure 2). The reasons for this are the subject of current investigations. DFS-QCPMG at 21.14 T has also been used to successfully examine the strontium-binding environment in a number of heat treated micas, montmorillonites, titanates, and titanosilicates. To perform such strontium-87 NMR analyses at more conventional fields (i.e., 11.74 T) would require on the order of 1800 days rather than the three days required to produce the spectrum shown in Figure 2. The library of quadrupolar parameters and their relationship to crystal structure prepared from our studies of simple systems now allows informed predictions of the strontium-binding environment based on strontium-87 NMR parameters and x-ray diffraction studies. This library could not have been developed over the past year without the use of DFS-QCPMG on the EMSL 21.14-T (900-MHz) NMR spectrometer. A detailed discussion of the strontium-binding environment in one of the mica samples mentioned earlier is the subject of a manuscript published in the *Journal of Physical Chemistry B* (Crosson et al. 2006). We also intend to publish the results of our mineral studies in a paper that will detail strontium binding in phyllosilicates and in another paper that will describe strontium binding in designer titanosilicate materials.

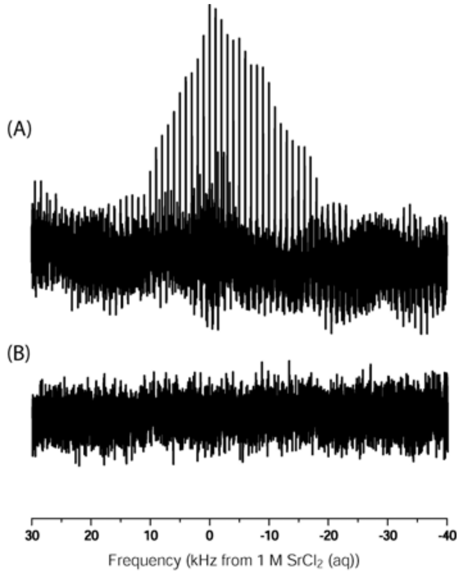

Figure 2. Strontium NMR spectra of Na-4 Mica after (A) and prior to (B) heat treatment at 500˚C for four hours. The heat-treated sample produces a single strontium resonance fit well by a quadrupolar line shape.

In the coming year, we intend to return to EMSL to study additional titanosilicate materials developed at Savannah River National Laboratory specifically to sequester strontium from Hanford-like wastes. Some of these materials have tunable selectivity for cesium and strontium, making this work highly important to the DOE mission. We will also continuing our investigations of mineral weathering under near-field exposure to simulated tank waste leachate (Chorover et al. 2003; Crosson et al. 2006) by monitoring the kinetics of mineral dissolution and re-precipitation in samples of natural Hanford sediments.

Citations

Bastow TJ. 2002. "Electric Field Gradients at the M-site in MCO3: M=Mg, Ca, Sr and Ba." *Chemical Physics Letters* 354(1-2):156-159.

Bowers GM, AS Lipton, and KT Mueller. 2006. "High-Field QCPMG NMR of Strontium Nuclei in Natural Minerals." *Solid State Nuclear Magnetic Resonance* 29(1-3):95-103.

Chorover J, SK Choi, MK Amistadi, KG Karthikeyan, G Crosson, and KT Mueller. 2003. "Linking Cesium and Strontium Uptake to Kaolinite Weathering in Simulated Tank Waste Leachate." *Environmental Science & Technology* 37(10):2200-2208.

Crosson GS, SK Choi, J Chorover, MK Amistadi, PA O'Day, and KT Mueller. 2006. "Solid-State NMR Identification and Quantification of Newly Formed Aluminosilicate Phases in Weathered Kaolinite Systems." *Journal of Physical Chemistry B* 110(2):723-732.

Larsen FH, J Skibsted, HJ Jakcobsen, and NC Nielsen. 2000. "Solid-state QCPMG NMR of Low-γ Quadrupolar Metal Nuclei in Natural Abundance." *Journal of the American Chemical Society* 122(29):7080-7086.

Identification of Functional Pathways Associated with Clinical Tamoxifen-Resistance in Breast Cancer by Advanced Mass Spectrometry

A Umar,(a) TM Luider,(a) JA Foekens,(a) and L Paša Tolić(b)

(a) Erasmus University Medical Center, Rotterdam, The Netherlands
(b) Pacific Northwest National Laboratory, Richland, Washington

Not all cancers respond equally to standard cancer drugs. If a doctor can determine how a cancer will respond to a drug before treatment begins, he will know if he has to prescribe an aggressive dose or a more modest one. By examining the proteins present in tumor samples from patients with a known response history, we can identify markers that will correlate with the response and aid doctors in prescribing the correct dose.

A Umar from the Erasmus University Medical Center in Rotterdam, The Netherlands, is visiting EMSL to characterize functional pathways that lead to clinical resistance to tamoxifen (anti-estrogen) treatment in breast cancer patients.

For this study, she has used laser microdissected tumor cells from patients that either were or were not responding to tamoxifen treatment. Protein profiles from these cells were generated by state-of-the-art nanoscale liquid chromatography Fourier transform infrared cyclotron resonance mass spectrometry (nLC-FTICR-MS), and the profiles were compared. Laser microdissection has the great advantage of enabling isolation of selected subpopulations of cells, such as tumor cells, and thus overcoming the issue of tissue heterogeneity. However, this process is very time consuming, so typically only a few thousand cells amounting to a few hundred nanograms of protein can be collected per tissue. Analysis of such minute amounts of sample by conventional proteomics tools is severely constrained by detection limits. As a consequence, ultra-sensitive nLC-FTICR technology developed at EMSL is the best choice for performing comprehensive proteome analyses. The nLC-FTICR-MS technique was applied to clinical samples and showed improved proteome coverage and good reproducibility attainable for ~3000 laser microdissected breast carcinoma cells as compared to what was previously described. As a next step, Umar used this approach to analyze 50 different tumor samples. She was able to detect protein profiles that were specifically expressed in either responding or nonresponding tumors (Figure 1). Validation of these protein profiles and further functional analysis of the proteins will eventually advance our understanding of breast cancer therapy-resistance and may lead the development of new and better therapies.

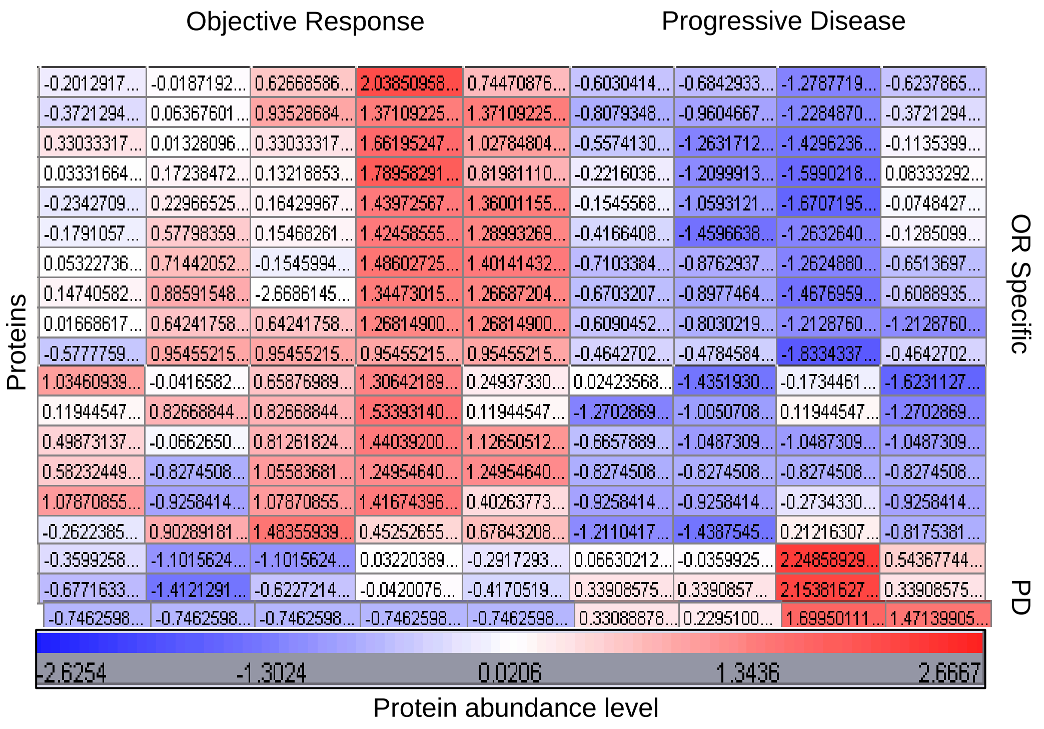

Objective Response					Progressive Disease			
-0.2012917...	-0.0187192...	0.62668586...	2.03850958...	0.74470876...	-0.6030414...	-0.6842933...	-1.2787719...	-0.6237865...
-0.3721294...	0.06367601...	0.93528684...	1.37109225...	1.37109225...	-0.8079348...	-0.9604667...	-1.2284870...	-0.3721294...
0.33033317...	0.01328096...	0.33033317...	1.66195247...	1.02784804...	-0.5574130...	-1.2631712...	-1.4296236...	-0.1135399...
0.03331664...	0.17238472...	0.13218853...	1.78958291...	0.81981110...	-0.2216036...	-1.2099913...	-1.5990218...	0.08333292...
-0.2342709...	0.22966525...	0.16429967...	1.43972567...	1.36001155...	-0.1545568...	-1.0593121...	-1.6707195...	-0.0748427...
-0.1791057...	0.57798359...	0.15468261...	1.42458555...	1.28993269...	-0.4166408...	-1.4596638...	-1.2632640...	-0.1285099...
0.05322736...	0.71442052...	-0.1545994...	1.48602725...	1.40141432...	-0.7103384...	-0.8762937...	-1.2624880...	-0.6513697...
0.14740582...	0.88591548...	-2.6686145...	1.34473015...	1.26687204...	-0.6703207...	-0.8977464...	-1.4676959...	-0.6088935...
0.01668617...	0.64241758...	0.64241758...	1.26814900...	1.26814900...	-0.6090452...	-0.8030219...	-1.2128760...	-1.2128760...
-0.5777759...	0.95455215...	0.95455215...	0.95455215...	0.95455215...	-0.4642702...	-0.4784584...	-1.8334337...	-0.4642702...
1.03460939...	-0.0416582...	0.65876989...	1.30642189...	0.24937330...	0.02423568...	-1.4351930...	-0.1734461...	-1.6231127...
0.11944547...	0.82668844...	0.82668844...	1.53393140...	0.11944547...	-1.2702869...	-1.0050708...	0.11944547...	-1.2702869...
0.49873137...	-0.0662650...	0.81261824...	1.44039200...	1.12650512...	-0.6657889...	-1.0487309...	-1.0487309...	-1.0487309...
0.58232449...	-0.8274508...	1.05583681...	1.24954640...	1.24954640...	-0.8274508...	-0.8274508...	-0.8274508...	-0.8274508...
1.07870855...	-0.9258414...	1.07870855...	1.41674396...	0.40263773...	-0.9258414...	-0.9258414...	-0.2734330...	-0.9258414...
-0.2622385...	0.90289181...	1.48355939...	0.45252655...	0.67843208...	-1.2110417...	-1.4387545...	0.21216307...	-0.8175381...
-0.3599258...	-1.1015624...	-1.1015624...	0.03220389...	-0.2917293...	0.06630212...	-0.0359925...	2.24858929...	0.54367744...
-0.6771633...	-1.4121291...	-0.6227214...	-0.0420076...	-0.4170519...	0.33908575...	0.3390857...	2.15381627...	0.33908575...
-0.7462598...	-0.7462598...	-0.7462598...	-0.7462598...	-0.7462598...	0.33088878...	0.2295100...	1.69950111...	1.47139905...

Figure 1. Detail of response-specific protein profile. Hierarchical clustering with z-scores was performed on 1999 proteins using protein abundance (obtained by averaging measured peptide abundances). The average protein abundance level (0.0206) is represented with a white background color, while the abundance levels above and below the average are represented by red and blue background colors,

Kinetics of Electron-Beam-Enhanced Recrystallization of Amorphous Strontium Titanate

***Y Zhang,*[a] *J Lian,*[b] *CM Wang,*[a] *RC Ewing,*[b] *and WJ Weber*[c]**

(a) W.R. Wiley Environmental Molecular Sciences Laboratory, Richland, Washington
(b) University of Michigan, Ann Arbor, Michigan
(c) Pacific Northwest National Laboratory, Richland, Washington

Single crystal strontium titanate ($SrTiO_3$) is of technological interest in microelectronics industries because of its high dielectric constant, good insulating properties, outstanding wear resistance, high oxidation resistance, and chemical and thermal stability. Strontium titanate thin films are used as insulating layers in dynamic random access memories, ferroelectric thin-film structures, and high-T_c superconductor devices, as well as potential gate oxide candidates. Strontium titanate and other titanate ceramics have also been proposed as phases for immobilization of nuclear waste. In many of these applications, knowledge of dynamic recovery and nanostructure evolution is critical.

Irradiation of $SrTiO_3$ with 1.0 MeV Au at 400 K leads to formation of an amorphous surface layer. In this research, the damage and microstructural features in the samples were investigated by Rutherford back-scattering spectroscopy and high-resolution transmission electron microscopy (TEM) images, and the results show amorphous regions of ~10.6 nm and ~330 nm for sample A, as shown in Figure 1(a), and sample B, respectively. Following exposure of the amorphous layers to TEM electron-beam (*e*-beam), the amorphous thickness decreases with exposure time, and *in situ* epitaxial recrystalli-zation at the amorphous/ crystalline (a/c) interface is observed, as shown in Figures 1(b) and 2. In the central area of the cross-sectional TEM image of sample A in Figure 1(b) where the *e*-beam is the most intense, more amorphous material recrystallizes, and the a/c interface moves toward the surface. At both edges of the cross-sectional image where the *e*-beam density is lower, recrystallization is not as significant. This indicates a strong dependence of the recrystallization process on *e*-beam flux. The *e*-beam-induced recrystallization of the amorphous layer in sample B is shown in Figure 2, where rapid *in situ* recrystallization at the a/c interface is evident.

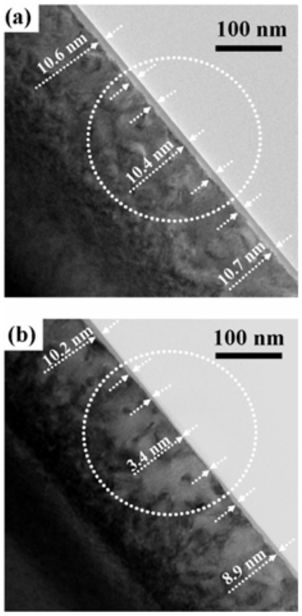

Figure 1. TEM images of sample A: (a) the amorphous layer. (b) recrystallization of amorphous layer following the *e*-beam irradiation.

The *in situ* recrystallization of the amorphous layer at room temperature under different beam flux is summarized in Figure 3. The solid phase regrowth appears as a series of linear stages with decreasing slopes as exposure time increases, resembling a sublinear-like regrowth behavior. In general, the recrystallization rate resulting from *e*-beam irradiation can be separated into three stages. During the initial stage (i.e., up to ~100 s), there exist many ion-induced defects near the a/c interface. Rapid motion at the a/c interface is observed, and the recrystallization processes proceed at a high rate. This fast recrystallization may be attributed to *e*-beam-enhanced defect annihilation at the a/c interface. Under the high *e*-beam flux (5.0 and 7.8 $\times 10^{20}$ $cm^{-2}s^{-1}$), the recrystallization processes during the initial stage occur very quickly, and no data were obtained during the very short durations. After the initial stage, during which most ion-induced defects were annealed out, the recrystallization rates become constant, and the recrystallization processes occur in a second stage. A well-defined linear relationship is observed for different fluxes at this stage. As the exposure time increases, little motion is observed at the a/c interface, and the recrystallization processes reach a saturation stage. The TEM observations indicate that the saturation stage occurs when the thickness of the amorphous layer is ~3 nm, which suggests that the surface may play an important role in stabilizing this final stage. It is evident in Figure 3 that the regrowth rate during the second stage increases with increasing beam flux from 1.2 to 5.0 $\times 10^{20}$ $cm^{-2}s^{-1}$, and shows no further increase with the increasing flux.

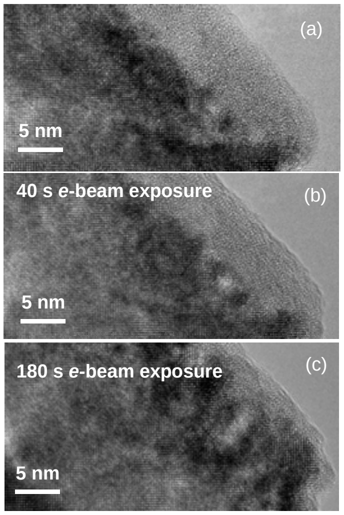

Figure 2. The a/c interface motion under *e*-beam exposure with flux of 5.0 $\times 10^{20}$ $cm^{-2}s^{-1}$.

The regrowth rates in the second linear stage under *e*-beam irradiation were investigated as a function of flux and temperature. The *e*-beam enhanced recrystallization rates are orders of magnitude higher than those expected from thermal epitaxial recrystallization. Based on the temperature dependence of the recrystallization rates, an activation energy of 0.1±0.05 eV was determined for the *e*-beam-enhanced recrystallization processes. A sublinear-like regrowth dependence on exposure time may be used as a fingerprint for the *e*-beam enhanced recrystallization, as opposed to the superlinear-like behavior normally observed in thermal recrystallization.

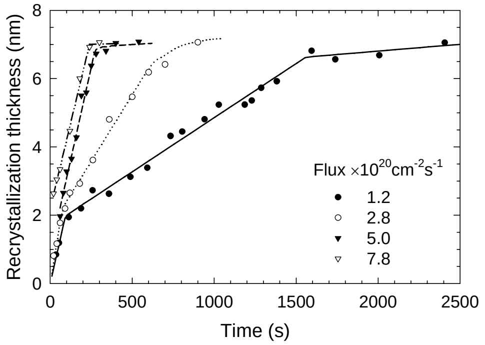

Figure 3. Solid phase regrowth of a/c transition as a function of exposure time to the *e*-beam under different fluxes.

During *e*-beam irradiation, the incident electrons primarily transfer energy by ionization processes that produce localized electronic excitations. The localized electronic excitations affect local atomic bonds and may effectively lower the energy barriers to recrystallization processes, which may involve local atomic hopping or rotation of atomic polyhedra.

Room-Temperature, Solvent-Free Synthesis of Monodisperse Magnetite Nanocrystals

XR Ye,[a] C Daraio,[a] CM Wang,[b] JB Talbot,[a] and S Jin[a]
(a) University of California-San Diego, La Jolla, California
(b) W.R. Wiley Environmental Molecular Science Laboratory, Richland, Washington

Magnetic nanoparticles are useful for a variety of scientific and technological applications such as magnetic storage media, ferrofluids, magnetic refrigeration, magnetic resonance imaging, hyperthermic cancer treatment, cell sorting, and targeted drug delivery. Iron oxides constitute one of the most fascinating classes of magnetic materials and have been extensively investigated. Based on chemical reactions in liquid or aerosol/vapor phases, different approaches such as coprecipitation, sol-gel, aging, ultrasound irradiation, and laser pyrolysis, have been established for preparing super-paramagnetic iron oxide nanoparticles typically smaller than 20 nm that are adaptable to variable applications. However, the relatively poor size uniformity and crystallinity of the nanoparticles obtained strongly affect their magnetic properties.

In this highlight, we report, for the first time, a novel, facile, and solvent-free synthetic method that allows the use of inorganic ferrous and ferric solids, along with surfactants, to produce monodisperse magnetite nanocrystals. The reaction is advantageous in that it is induced at room temperature rather than at the refluxing temperatures of ~265 to 350°C used in the typical organic-solution phase decomposition method in which organic iron is dissolved in organic solvents. Highly crystalline and monodispersed Fe_3O_4 nanocrystalline particles are obtained by the new process despite the fact that the reaction occurs at room temperature. Such a solvent-free reaction provides a substantial environmental advantage in that it eliminates the need

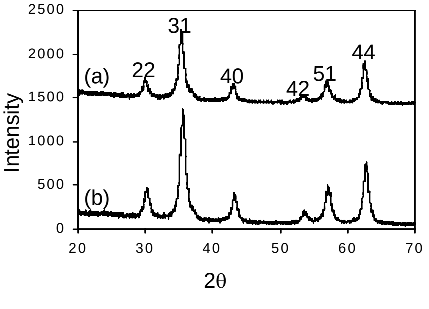

Figure 1. X-ray diffraction patterns of the nanoparticles.

for disposing of or recycling toxic chemicals. A solvent-free approach based on solid-state reactions was previously used for simple synthesis of unassembled nanoparticles; however, no surfactant was used for particle size control.

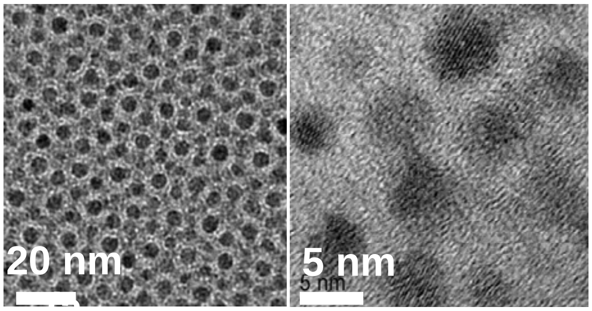

Figure 2. Transmission electron micrographs

Solvent-free synthesis of magnetite nanocrystals can be considered as a hybrid of solid-state reaction, co-precipitation, and organic solution-phase decomposition processes that take advantage of only the beneficial parts of these processes. In this approach, the following modifications were made: 1) inorganic ferrous, ferric, and base solids were used directly for the synthesis rather than aqueous or organic solutions; 2) an oleic acid-oleylamine adduct solid was used as the surfactant stabilizer rather than oleic acid and oleylamine liquids; 3) after the reaction, the Fe_3O_4 nanoparticles were extracted directly into hexane, and the unreacted materials and the byproducts were separated conveniently since they are insoluble in hexane; and 4) mono-dispersed, uniform Fe_3O_4 nanoparticles that can be assembled into ordered arrays were obtained. In addition, this method requires no complex apparatus and techniques, and enables one to synthesize Fe_3O_4 nanocrystals with almost uniform size in high yields and at a large scale. The reaction, if carried out in the presence of a surfactant such as oleic acid-oleylamine adduct, generated monodisperse Fe_3O_4 nanocrystals extractable directly from the reaction mixture. The extracted nanoparticles were capable of forming a self-assembled, two-dimensional, and uniform periodic array. The new process uses inexpensive and nontoxic starting materials, and does not require a use of high-boiling-point toxic solvents, so it is amenable to an environmentally desirable, large-scale synthesis of nanocrystals.

X-ray diffraction patterns of the nanoparticles synthesized by the solvent-free reactions with and without the addition of oleic acid-oleylamine adduct are compared in Figure 1. Both patterns indicate the crystalline nature of the products, and the positions and relative intensities of all diffraction peaks coincide with those of the Joint Committee for Powder Diffraction Studies card (19-0629) for Fe_3O_4. No characteristic peaks of reactants and byproducts (mostly NaCl) were observed. The general transmission electron micrograph of the nanoparticles synthesized by the solvent-free reaction in the presence of surfactant is shown in Figure 2 (left image). The nanoparticles appear almost spherical and monodispersed with an average diameter of 5 nm, and self assemble into a two-dimensional array. A high-resolution transmission electron micrograph of the patterned nanoparticles is shown in Figure 2 (right image). The lattice spacing seen in the lattice fringe of the particles revealed the satisfactory crystallinity and structural uniformity of the sample.

We have successfully demonstrated and documented the synthesis of monodisperse Fe_3O_4 nanocrystals using a novel and easy one-step, solvent-free reaction (Ye et al. 2006). The reaction of the solvent-free synthesis in the presence of a surfactant is believed to precede a similar intermediate process via the formation of Fe(III) and Fe(II)-surfactant complexes. The reaction can be conveniently carried out at ambient temperature, thereby avoiding the use of toxic solvents with high boiling points. This technique, which uses inexpensive and nontoxic inorganic ferrous and ferric salts that are reacted at ambient temperature, is amenable to convenient, large-scale synthesis. With proper choices of inorganic metal salts and surfactants, this method may be extended to environmentally desirable preparation of a wide variety of monodisperse nanocrystals.

This research is described in more detail in Ye et al. 2006.

Citation

Ye X, C Daraio, C Wang, JB Talbot, and S Jin. 2006. “Room Temperature Solvent-Free Synthesis of Monodisperse Magnetite Nanocrystals.” *Journal of Nanoscience and Nanotechnology* 6(3):852-856.

MSCF Users Leading the Way to Zero Emission Transportation

J Li[a] *and MS Gutowski*[b]

(a) W.R. Wiley Environmental Molecular Sciences Laboratory, Richland, Washington

(b) Pacific Northwest National Laboratory, Richland Washington

Hydrogen fuel cells are an environmentally friendly way to power vehicles. Recent years have seen increasing interest for research on efficient hydrogen fuel cells from the federal government and the transportation industry. The main challenge today for energy industries is how to make hydrogen fuel cells economically competitive with their conventional fuel counterparts. A key issue that must be addressed is the efficient storage of hydrogen, which would allow hydrogen-powered cars to cover longer distances on a single “tank” and fuel distributors to efficiently deliver hydrogen to consumers.

The idea of “zero-emission” transportation has long been a dream for protecting the environment. Hydrogen-powered cars would bring that dream a step closer to becoming an economically viable alternative to conventional transportation fuels. Many research efforts focus on hydrogen fuel cells; however, hydrogen storage is a key bottleneck to implementing this approach. While highly compressed hydrogen gas and liquefied hydrogen are unlikely to be of sufficient volumetric density, the use of chemical hydrogen storage materials based on light elements is possibly a feasible approach. Recently a joint computational and experimental research project, led by PNNL scientists M Gutowski and T Autrey, has made important progress on ammonia borane (BH_3NH_3)-based materials, which hold great promise for hydrogen storage (Gutowski and Autrey 2006). The computational research of this project is part of the Molecular Science Computing Facility Computational Grand-Challenge 9601 (Computational Design of Materials for Hydrogen Storage, PI: Jonnson), which is one of the computational projects supported by the EMSL.

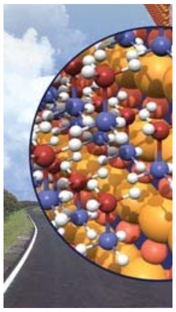

-
- **Figure 1.** Ammonia borane materials consist of interlocking networks of ammonia and borane units, which form a structural and electrical scaffolding that can hold hydrogen.

The main challenges for making hyrdogen fuel cells competitive with conventional fuel involve scale. A viable hydrogen storage medium would have to optimize the density of hydrogen while maintaining favorable electrical and thermodynamic properties. For ammonia borane compounds, the density of hydrogen storage is between 19% and 24%, which make these materials excellent study candidates for hydrogen storage. The computational simulation work has demonstrated that for a variety of ammonia borane materials, the release of hydrogen is for the most part thermodynamically neutral (i.e., the release and uptake of hydrogen from the material is nearly reversible at equilibrium). Currently, removing hydrogen from ammonia borane materials has been shown to be feasible at relatively low temperatures, which is an important characteristic for making hydrogen fuel cells practical in vehicles. However, a significant challenge still exists in that there is a large energy barrier associated with "filling" ammonia borane materials with hydrogen. This energy barrier represents a practical limitation in that to be competitive, distribution of alternative fuels to consumers must be easy. Future work from this Grand Challenge will focus, in part, on searching for a solution to this limitation for ammonia borane materials. If successful, this project could help pave the way to zero-emission transportation fuels that would revolutionize the automobile industry and have a significant impact on providing a solution for achieving and sustaining a clean environment.

Citation

Gutowski MS and T Autrey. 2006. "Hydrogen Gets Onboard." *Chemistry World* 3(3):44-48.

Using Advanced Statistical Models to Improve High-Throughput Proteomics

W Cannon[(a)] *and DJ Baxter*[(b)]

(a) Pacific Northwest National Laboratory, Richland, Washington

(b) W.R. Wiley Environmental Molecular Sciences Laboratory, Richland, Washington

Genes are DNA segments that when "turned on" provide living cells with instructions on how to build proteins, which are molecules that can be used as the cellular "skeleton," allow some cells to move, process energy and waste products, and participate in virtually every function required for cells to live. Understanding how organisms work requires us to get a detailed picture of the proteins inside them. High-throughput proteomics is a rapid way to measure the protein content of biological samples, but the veracity of those measurements is, in part, determined by the rate of correctly identifying proteins or protein pieces.

Detecting bioterrorism threats, ensuring a safe food supply, and using microbes to clean up the environment or as a "clean" energy source are just some of the areas of biology where rapidly analyzing very large collections of proteins, or working molecules is a key technology. High-throughput proteomics is a signature capability at PNNL, where the capability is made available to a worldwide community of users to rapidly identify all the proteins in a biological sample. Reliably identifying the protein content of a cell gives important information about its function, making it possible to develop new ways in which cells can easily be identified, which is important in detecting bio-threats.

The main computational challenge associated with high-throughput proteomics is the task of identifying protein fragments (peptides) from measurements of the mass-to-charge ratio (m/z) of small pieces of the peptides. In a high-throughput method known as tandem mass spectrometry (MS/MS), this collection of m/z values can be used as a mass fingerprint to identify the correct peptide sequence from a large list of candidate peptides. *Polygraph*, a high-performance application designed to perform this peptide identification task, has been demonstrated to improve the identification rate of peptides measured by MS/MS. This performance improvement is achieved, in part, by using an advanced statistical model to better understand and identify the fingerprint associated with each peptide. Previous methods generally worked under the assumption that peptides are equally likely to fragment anywhere along their length. However, measurements of the probability of fragmentation along the peptide have shown that there is a strong position-dependence to the likelihood of fragmentation (Figure 1). Including this additional information into *Polygraph* has resulted in a substantial improvement in the ability to correctly identify peptides.

Future directions of this Computational Grand-Challenge 9603 research include development of a data-intensive version of *Polygraph* that would reduce by a factor of one-third the time required to accurately identify peptides from MS/MS data.

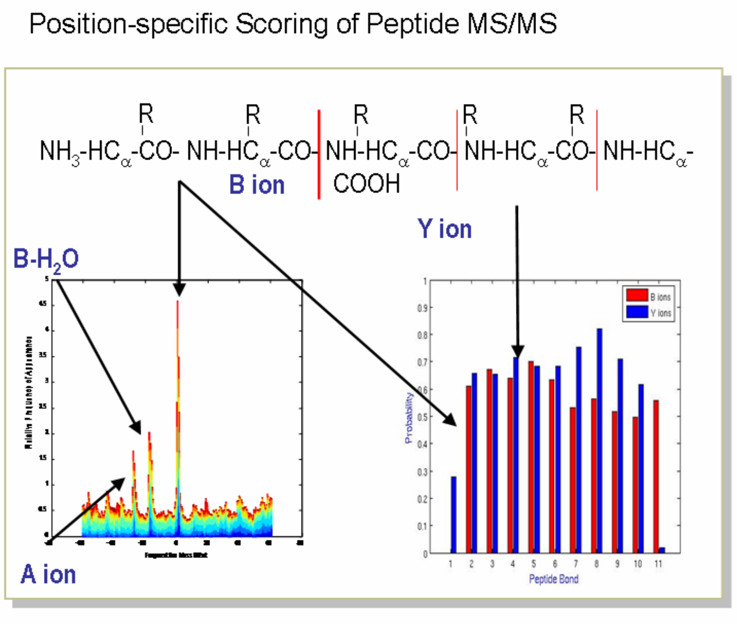

Figure 1. Using a position-dependent description of likelihood of peptide fragmentation has resulted in a fourfold reduction in the false positive identification rate.

Publications Resulting From This Grand Challenge and Pilot Project

Cannon WR and KD Jarman. 2003. "Improved Peptide Sequencing Using Isotope Information Inherent in Tandem Mass Spectra." *Rapid Communications in Mass Spectrom*etry 17(15)1793-1801.

Cannon WR, KH Jarman, BM Webb-Robertson, DJ Baxter, CS Oehmen, KD Jarman, A Heredia-Langner, KJ Auberry, and GA Anderson. 2005. "A Comparison of Probability and Likelihood Models for Peptide Identification from Tandem Mass Spectrometry Data." *Journal of Proteome Research* 4(5):1687-1698.

Heredia-Langner A, WR Cannon, KD Jarman, and KH Jarman. 2004. "Sequence Optimization as an Alternative to *De Novo* Analysis of Tandem Mass Spectrometry Data." *Bioinformatics.* 20(14):2296-2304.

Jarman KD, WR Cannon, KH Jarman, and A Heredia-Langner. 2003. "A Model of Random Sequences for *De Novo* Peptide Sequencing." In *Proceedings of the 3rd IEEE International Symposium on Bioinformatics and Bioengineering*, pp. 206-213, IEEE Computer Society, Los Alamitos, California.

Malard JM, A Heredia-Langner, DJ Baxter, KH Jarman, and WR Cannon. 2004. "Constrained *De Novo* Peptide Identification via Multi-Objective Optimization." In *Proceedings of the 18th International Parallel and Distributed Processing Symposium*, pp. 191-199, IEEE Computer Society, Los Alamitos, California.

Malard JM., A Heredia-Langner, WR Cannon, RW Mooney, and DJ Baxter. 2005. "Peptide Identification via Constrained Multi-Objective Optimization: Pareto-Based Genetic Algorithms." *Concurrency and Computation: Practice and Experience* 17(14)1687-1704.

Awards and Recognition

EMSL User Honored by AAAS. EMSL user Bruce Kay (PNNL) was inducted as a Fellow in the American Association for the Advancement of Science, which cited his "meritorious efforts to advance science or its applications."

EMSL Staff and Users Recognized by PNNL. On April 12, 2006, 22 EMSL staff members and resident users were honored by the PNNL for their scientific contributions. The contributions cited included receiving patents for original ideas, developing software, contributing to technology commercialization, and receiving prestigious scientific awards.

EMSL User Appointed to ASMS Board of Directors. EMSL user Julia Laskin (PNNL) has been appointed to the American Society for Mass Spectrometry Board of Directors. Laskin will act as treasurer of the Board. In this role, she will make recommendations to the Board relevant to preserving the economic health of the Society and will present a financial report at each annual meeting.

Professional/Community Service

On March 30, 2006, students and faculty of Washington State University-Tri-Cities, Richland, Washington, visited the EMSL High-Field Magnetic Resonance Facility. The students ran NMR experiments related to their coursework. EMSL staff members Joe Ford and Sarah Burton hosted the visit.

On April 25, 2006, seven students and a chemistry professor from Columbia Basin College/Washington State University visited the EMSL High-Field Magnetic Resonance Facility. The students ran NMR experiments related to their instrumental analysis coursework. EMSL staff member Sarah Burton hosted the visit.

EMSL user Mike Bowman (Pacific Northwest National Laboratory) traveled to Washington State University, Pullman Washington, to serve on a Thesis Defense Committee. He participated in the doctoral thesis defense of Dr. Jonathan Cape. Cape's thesis topic was "The Mechanism of Quinol Oxidation in the Cytochrome bc complex." This doctoral defense included work performed as a user in the EMSL High-Field Magnetic Resonance Facility.

Visitors and Users

A total of 392 users used the capabilities of EMSL during this reporting period, with 244 visiting onsite and 148 using capabilities remotely.

Publications

The following list represents publications by EMSL staff members and users where the publication resulted from research carried out in EMSL.

Alam TM, BR Cherry, KR Minard, and M Celina. 2005. "Relaxation Nuclear Magnetic Resonance Imaging Investigation of Heterogeneous Aging in a Hydroxy-Terminated Polybutadiene-Based Elastomer." *Macromolecules* 38(26):10694-10701.

Bowers GM, R Ravella, S Komarneni, and KT Mueller. 2006. "NMR Study of Strontium Binding by a Micaceous Mineral." *Journal of Physical Chemistry B* 110(14):7159-7164.

Bryantsev V and BP Hay. 2006. "Conformational Preferences and Internal Rotation in Alkyl- and Phenyl-Substituted Thiourea Derivatives." *Journal of Physical Chemistry A* 110(14):4678-4688.

Brzovic PS, J O'Keeffe, DE Christensen, DW Hoyt, and RE Klevit. 2006. "A UbcH5/Ubiquitin Noncovalent Complex is Required for Processive BRCA1-Directed Ubiquitination." *Molecular Cell* 12(6): 873-880.

Cho HM, AR Felmy, RN Craciun, JP Keenum, NK Shah, and DA Dixon. 2006. "Solution State Structure Determination of Silicate Oligomers by ^{29}Si NMR Spectroscopy and Molecular Modeling." *Journal of the American Chemical Society* 128(7):2324-2335. doi:10.1021/ja0559202

Craig NC, MC Moore, AK Patchen, and RL Sams. 2006. "Analysis of Rotational Structure in the High-Resolution Infrared Spectrum and Assignment of Vibrational Fundamentals of Butadiene-2,3-C-13(2)." *Journal of Molecular Spectroscopy* 235(2):181-189.

Dohnalek Z, J Kim, O Bondarchuk, JM White, and BD Kay. 2006. "Physisorption of N_2, O_2, and CO on Fully Oxidized TiO_2(110)." *Journal of Physical Chemistry B* 110(12):6229-6235. doi:10.1021/jp0564905

El-Shafey A, N Tolic, MM Young, KL Sale, RD Smith, and V Kery. 2006. "Zero-Length Cross-Linking in Solid State as an Approach for Analysis of Protein-Protein Interactions." *Protein Science* 15(3):429-440.

Fan P and S Hirata. 2006. "Active-Space Coupled-Cluster Methods through Connected Quadruple Excitations." *Journal of Chemical Physics* 124:104108-104117.

Fang R, DA Elias, ME Monroe, Y Shen, M McIntosh, P Wang, CD Goddard, SJ Callister, RJ Moore, YA Gorby, JN Adkins, JK Fredrickson, MS Lipton, and RD Smith. 2006. "Differential Label-Free Quantitative Proteomic Analysis of *Shewanella oneidensis* Cultured under Aerobic and Suboxic Conditions by Accurate Mass and Time Tag Approach." *Molecular & Cellular Proteomics* 5:714-725. doi:10.1074/mcp. M500301-MCP200

Felmy AR, HM Cho, DA Dixon, Y Xia, NJ Hess, and Z Wang. 2006. "The Aqueous Complexation of Thorium with Citrate under Neutral to Basic Conditions." *Radiochimica Acta* 94(4):205-212. doi:10.1524/ract.2006.94.4.205

Felmy AR, EJ Bylaska, DA Dixon, M Dupuis, JW Halley, R Kawai, KM Rosso, JR Rustad, PE Smith, T Straatsma, GA Voth, JH Weare, and DA Yuen. 2006. *Computational Studies in Molecular Geochemistry and Biogeochemistry*. PNNL-15462, Pacific Northwest National Laboratory, Richland, Washington.

Fir B, M Whalen, H Mercier, DA Dixon, and GJ Schrobilgen. 2006. "Syntheses of $[F_5TeNH_3][AsF_6]$, $[F_5TeN(H)Xe][AsF_6]$, and F_5TeNF_2 and Characterization by Multi-NMR and Raman Spectroscopy and by Electronic Structure Calculations: The X-ray Crystal Structures of α- andβ-F_5TeNH_2, $[F_5TeNH_3][AsF_6]$, and $[F_5TeN(H)Xe][AsF_6]$." *Inorganic Chemistry* 45(5):1978-1996.

Fox PM, JA Davis, and JM Zachara. 2006. "The Effect of Calcium on Aqueous Uranium (VI) Speciation and Adsorption to Ferrihydrite and Quartz." *Geochimica et Cosmochimica Acta* 70(6):1379-1387.

Francisco JS, SM Kathmann, GK Schenter, LX Dang, SS Xantheas, BC Garrett, S Du, DA Dixon, R Bianco, S Wang, JT Hynes, A Morita, and KA Peterson. 2006. *A Computational Approach to Understanding Aerosol Formation and Oxidant Chemistry in the Troposphere.* PNNL-15772, Pacific Northwest National Laboratory, Richland, Washington.

Gallagher NB, TA Blake, and PL Gassman. 2005. "Application of Extended Inverse Scatter Correction to Mid-Infrared Reflectance Spectra of Soil." *Journal of Chemometrics* 19(5-7):271-281. doi:10.1002/cem.929

Groenewold GS, AK Gianotto, KC Cossel, MJ Van Stipdonk, DT Moore, N Polfer, J Oomens, WA De Jong, and L Visscher. 2006. "Vibrational Spectroscopy of Mass-Selected [UO_2(ligand)n]2+ Complexes in the Gas Phase: Comparison with Theory." *Journal of the American Chemical Society* 128:4802-4813.

Gun'ko VM, VV Turov, V Barvinchenko, VM Bogatyrev, AV Turov, OV Shulga, O Stebelska, V Pokrovsky, R Leboda, V Sukretny, Y Nychiporuk, Y Gornikov, B Chuikov, and Y Ptushinskii. 2006. "Characteristics of Interfacial Water at Nanosilica Surface with Adsorbed 1,3,5-Trihydroxybenzene Over Wide Temperature Range." *Colloids and Surfaces A, Physicochemical and Engineering Aspects* 278:106-122.

Herrera JE, J K Wak, J Hu, Y Wang, CH Peden, J Macht, and E Iglesia. 2006. "Synthesis, Characterization, and Catalytic Function of Novel Highly Dispersed Tungsten Oxide Catalysts on Mesoporous Silica." *Journal of Catalysis* 239(1):200-211.

Hu J, RA Wind, and DN Rommereim. 2006. "H-1 Relaxation Times of Metabolites in Biological Samples Obtained with Nondestructive Ex-Vivo Slow-MAS NMR ." *Magnetic Resonance in Chemistry* 44(3):269-275. doi:10.1002/mrc.1764

Jackson SM. 2006. "Allocation Management Solutions for High Performance Computing." In *Proceedings of the 2005 International Conference on Parallel and Distributed Processing Techniques and Applications* 1-3:10-16, CSREA Press, Athens, Greece.

Jiang W, V Shutthanandan, Y Zhang, S Thevuthasan, WJ Weber, and GJ Exarhos. 2006. "Hydrogen Behavior in Mg^+-Implanted Graphite." *Journal of Materials Research* 21(4):811-815. doi:10.1557/JMR.2006.0121

Johnson TJ, T Masiello, and SW Sharpe. 2006. "The Quantitative Infrared and NIR Spectrum of CH2I2 Vapor: Vibrational Assignments and Potential for Atmospheric Monitoring." *Atmospheric Chemistry and Physics* 6:1275-1299.

Joly AG, JR Williams, SA Chambers, G Xiong, WP Hess, and DM Laman. 2006. "Carrier Dynamics in α-Fe_2O_3(0001) Thin Films and Single Crystals Probed by Femtosecond Transient Absorption and Reflectivity." *Journal of Applied Physics* 99(5):053521 (6 pages).

Kaspar TC, TC Droubay, V Shutthanadan, SM Heald, CM Wang, DE McCready, S Thevuthasan, JD Bryan, DR Gamelin, AJ Kellock, MF Toney, X Hong, C Ahn, and SA Chambers. 2006. "Ferromagnetism and Structure of Epitaxial Cr-doped Anatase TiO_2 Thin Films." *Physical Review. B, Condensed Matter and Materials Physics* 73(15):155327 (12 pages). doi:10.1103/PhysRevB.73.155327

Keske JC, W Lin, WC Pringle, SE Novick, TA Blake, and DF Plusquellic. 2006. "High-Resolution Studies of Tropolone in the S_0 and S_1 Electronic States: Isotope Driven Dynamics in the Zero-Point Energy Levels." *Journal of Chemical Physics* 124(7):074309 (pages 1-12).

Kiebel GR, KJ Auberry, N Jaitly, DA Clark, ME Monroe, ES Peterson, N Tolic, GA Anderson, and RD Smith. 2006. "PRISM: A Data Management System for High-Throughput Proteomics." *Proteomics* 6(6):1783-1790, doi: 10.1002/pmic.200500500.

Kittle-Godfrey A and M Cafiero. 2006. "Properties, Dynamics, and Electronic Structure of Atoms and Molecules Evaluation of DFT Methods for Computing the Interaction Energies of Homomolecular and Heteromolecular Dimers of Monosubstituted Benzene." *International Journal of Quantum Chemistry* 106(9): 2035-2043.

Kugai J, V Subramani, C Song, MH Engelhard, and Y Chin. 2006. "Effects of Nanocrystalline CeO_2 Supports on the Properties and Performance of Ni–Rh Bimetallic Catalyst for Oxidative Steam Reforming of Ethanol." *Journal of Catalysis* 238(2):430-440. doi:10.1016/j.jcat.2006.01.001

Laskin J, TH Bailey, and JH Futrell. 2006. "Mechanisms of Peptide Fragmentation from Time- and Energy-Resolved Surface-Induced Dissociation Studies: Dissociation of Angiotensin Analogs." *International Journal of Mass Spectrometry* 249:462-472.

Lin YC, D Sundholm, J Juselius, LF Cui, X Li, HJ Zhai, and LS Wang. 2006. "Experimental and Computational Studies of Alkali-Metal Coinage-Metal Clusters." *Journal of Physical Chemistry A* 110(12): 4244-4250.

Liu G and Y Lin. 2006. "Carbon Nanotube Templated Assembly of Protein." *Journal of Nanoscience and Nanotechnology* 6(4):948-953.

Matulis VE and OA Ivaskevich. 2006. "Comparative DFT Study of Electronic Structure and Geometry of Copper and Silver Clusters: Interaction with NO Molecule." *Computational Materials Science* 35(3):261-271.

Moision RM and PB Armentrout. 2006. "The Special Five-Membered Ring of Proline: An Experimental and Theoretical Investigation of Alkali Metal Cation Interactions with Proline and Its Four- and Six-Membered Ring Analogues." *Journal of Physical Chemistry A* 110:3933-3946.

Nielsen I and MD Allendorf. 2006. "Thermochemistry of the Chromium Hydroxides Cr(OH)n, n = 2-6, and the Oxyhydroxide CrO(OH): *Ab Initio* Predictions." *Journal of Physical Chemistry A* 110:4093-4099.

Nieplocha J, BJ Palmer, V Tipparaju, M Krishnan, HE Trease, and E Apra. 2006. "Advances, Applications, and Performance of the Global Arrays Shared Memory Programming Toolkit." *International Journal of High Performance Computing Applications* 20(2):230-231.

Page JS, AV Tolmachev, K Tang, and RD Smith. 2006. "Theoretical and Experimental Evaluation of the Low M/Z Transmission of an Electrodynamic Ion Funnel." *Journal of the American Society for Mass Spectrometry* 17(4):586-592.

Pan DH, N Klymyshyn, DH Hu, and HP Lu. 2006. "Tip-Enhanced Near-Field Raman Spectroscopy Probing Single Dye-Sensitized TiO_2 Nanoparticles." *Applied Physics Letters* 88(9):093121 (pages 1-3).

Pophristic V, S Vemparala, I Ivanov, Z Liu, ML Klein, and WF DeGrado. 2006. "Controlling the Shape and Flexibility of Arylamides: A Combined *Ab Initio*, *Ab Initio* Molecular Dynamics, and Classical Molecular Dynamics Study." *Journal of Physical Chemistry B* 110:3517-3526.

Raugei S and P Carloni. 2005. "Structure and Function of Vanadium Haloperoxidases." *Journal of Physical Chemistry* B 110(8):3747-3758. doi:10.1021/jp054901b

Roberts AG, MD Diaz, JN Lampe, LM Shireman, JS Grinstead, MJ Dabrowski, JT Pearson, MK Bowman, WM Atkins, and AP Campbell. 2006. "NMR Studies of Ligand Binding to P450eryF Provides Insight into the Mechanism of Cooperativity." *Biochemistry* 45(6):1673-1684.

Roh H, Y Wang, DL King, A Platon, and Y Chin. 2006. "Low Temperature and H_2 Selective Catalysts for Ethanol Steam Reforming." *Catalysis Letters* 108(1-2):15-19.

Salcedo D, TB Onasch, K Dzepina, MR Canagaratna, Q Zhang, JA Huffman, PF DeCarlo, JT Jayne, P Mortimer, DR Worsnop, CE Kolb, KS Johnson, B Zuberi, LC Marr, R Volkamer, LT Molina, MJ Molina, B Cardenas, RM Bernabe, C Marquez, JS Gaffney, NA Marley, A Laskin, V Shutthanandan, Y Xie, W Brune, R Lesher, T Shirley, and JL Jimenez. 2006. "Characterization of Ambient Aerosols in Mexico City during the MCMA-2003 Campaign with Aerosol Mass Spectrometry: Results from the CENICA Supersite." *Atmospheric Chemistry and Physics* 6:925-946.

Sanchez-Mori P, AJ Cohen, and W Yang. 2006. "Self-Interaction-Free Exchange-Correlation Functional for Thermochemistry and Kinetics." *Journal of Chemical Physics* 124(9):91102 (4 pages).

Saraf LV, DE McCready, V Shutthanandan, CM Wang, MH Engelhard, and S Thevuthasan. 2006. "Correlation Among Channeling, Morphological, and Micro-structural Properties in Epitaxial CeO_2 Films." *Electrochemical and Solid-State Letters* 9(5):J17-J20. doi:10.1149/1.2186029

Schryver JC, CC Brandt, SM Pfiffner, T Palumbo, AD Peacock, DC White, JP McKinley, and PE Long. 2006. "Application of Nonlinear Analysis Methods for Identifying Relationships between Microbial Community Structure and Groundwater Geochemistry." *Microbial Ecology* 51(2006):177-188. doi:10.1007/s00248-004-0137-0

Seabaugh JL, H Dong, RK Kukkadapu, DD Eberl, JP Morton, and J Kim. 2006. "Microbial Reduction of Fe(III) in the Fithian and Muloorina Illites: Contrasting Extents and Rates of Bioreduction." *Clays and Clay Minerals* 54(1):67-79. doi:10.1346/CCMN.2006.0540109

Shishkin O, GV Palamarchuk, L Gorb, and J Leszczynski. 2006. "Intramolecular Hydrogen Bonds in Canonical 2'-Deoxyribonucleotides: An Atoms in Molecules Study." *Journal of Physical Chemistry B* 110: 4413-4422.

Smith RS, T Zubkov, and BD Kay. 2006. "The Effect of the Incident Collision Energy on the Phase and Crystallization Kinetics of Vapor Deposited Water Films." *Journal of Chemical Physics* 124(11):114710 (pages 1-7).

Straatsma T, JA McCammon, JH Miller, PE Smith, ER Vorpagel, CF Wong, and M Zacharias. 2006. *Biomolecular Simulation of Base Excision Repair and Protein Signaling.* PNNL-15687, Pacific Northwest National Laboratory, Richland, Washington.

Sturdy YK, C Skylaris, and DC Clary. 2005. "Torsional Anharmonicity in the Conformational Analysis of β-D-Galactose." *Journal of Physical Chemistry B* 110:3485-3492.

Vayner G, Y Alexeev, J Wang, TL Windus, and WL Hase. 2006. "*Ab Initio* and Analytic Intermolecular Potentials for Ar-CF_4." *Journal of Physical Chemistry A* 110(9):3174-3178.

Vemparala S, I Ivanov, V Pophristic, and K Spiegel. 2006. "*Ab Initio* Calculations of Intramolecular Parameters for a Class of Arylamide Polymers." *Journal of Computational Chemistry* 27(6):693-700.

Wang J, G Liu, and Y Lin. 2006. "Amperometric Choline Biosensor Fabricated through Electrostatic Assembly of Bienzyme/Polyelectrolyte Hybrid Layers on Carbon Nanotubes." *Analyst* 131(4):477-483. doi: 10.1039/b516038c

Waters T, HK Woo, XB Wang, and LS Wang. 2006. "Probing the Intrinsic Electronic Structure of the Bis(dithiolene) Anions [M(mnt)(2)](2-) and [M(mnt)(2)](1-) (M = Ni, Pd, Pt; mnt=1,2-S2C2(CN)(2)) in the Gas Phase by Photoelectron Spectroscopy." *Journal of the American Chemical Society* 128(13):4282-4291.

Xia Y, NJ Hess, and AR Felmy. 2006. "Stability Constants of Technetium (IV) Oxalate Complexes as a Function of Ionic Strength." *Radiochimica Acta* 94(3):137-141. doi:10.1524/ract.2006.94.3.137

Xiao HY, X Zu, Y Zhang, and F Gao. 2006. "Atomic and Electronic Structures of Rubidium Adsorption on Si(001)(2 x 1) Surface: Comparison with Cs/Si(001) Surface." *Chemical Physics* 323(2-3):383–390. doi:10.1016/j.chemphys.2005.10.003

Xiong G, AG Joly, KM Beck, WP Hess, MD Cai, SC Langford, and JT Dickinson. 2006. "*In Situ* Photoelectron Emission Microscopy of a Thermally Induced Martensitic Transformation in a CuZnAl Shape Memory Alloy." *Applied Physics Letters* 88(9):091910 (pages 1-3).

Zhang ZR, O Bondarchuk, JM White, BD Kay, and Z Dohnalek. 2006. "Imaging Adsorbate O-H Bond Cleavage: Methanol on TiO_2(110)." *Journal of the American Chemical Society* 128(13):4198-4199.

Zheng F, DL Baldwin, LS Fifield, NC Anheier, Jr., CL Aardahl, and JW Grate. 2006. "Single-Walled Carbon Nanotube Paper as a Sorbent for Organic Vapor Preconcentration." *Analytical Chemistry* 78(7):2442-2446.

Zubarev DY, AN Alexandrova, AI Boldyrev, LF Cui, X Li, and LS Wang. 2006. "On the Structure and Chemical Bonding of Si_6^{2-} and Si_6^{2-} in $NaSi_6^-$ upon Na^+ Coordination." *Journal of Chemical Physics* 124(12):124305 (pages 1-13).

Presentations

During this reporting period, EMSL staff presented on research performed at the user facility at the following meetings or locations:

- 45th Sanibel Symposium
- 231st American Chemical Society National Meeting and Exposition

- 2006 Materials Research Society Meeting
- American Physical Society March Meeting
- High-Performance Computing-3 Project Plan Review
- International Data Group High-Performance Computing Forum
- Itanium Conference and Exposition 2006
- Moving the Laboratory Online: Practical Techniques for Utilizing Remote Instrumentation to Enhance Science Education (online conference)
- Scientific Computing Magazine Webcast: Power Up/Cool Down (online conference)
- U.S. Department of Energy 2006 Cyber Security Training Conference.